A MODULAR OPTICS DESIGN FOR THE LBNE BEAMLINE

JOHN A. JOHNSTONE

FERMILAB/APC/LBNE
10.22.2010

Protons extracted from the Main Injector (MI) in the MI-60 straight section are transported 84 m through quadrupole Q106 in the NuMI stub, at which point two 6-3-120 vertical switching magnets, followed by three EPB vertical dipoles, steer the beam into the main body of the LBNE beamline. From Q106 in NuMI the LBNE beamline transports these protons 722.0 m to the LBNE target, located 41.77 m (137.0 ft) below the MI beamline center (BLC) elevation, on a trajectory aimed towards DUSEL. Bending is provided (predominantly) by 34 long (6 m) MI-style IDA/IDB and 8 short (4 m) IDC/IDD dipoles [1] [through 48.36° horizontally and -5.844° (net) vertically]. Optical properties are defined by 49 quadrupoles (grouped functionally into 44 focusing centers) of the proven MI beamline-style 3Q60/3Q120 series [2]. All focusing centers are equipped with redesigned MI-style IDS orbit correctors [3] and dual-plane beam position monitors (BPM's) [4]. Ample space is available in each arc cell to accommodate ion pumps and diagnostic instrumentation. Parameters of the main magnets are listed in Table 1.

Optics

This 60-120 GeV/c transfer line design is comprised of distinct optical modules, as illustrated in Figure 1:

- A matching section between NuMI and main body of the LBNE FODO lattice
- A periodic section of 4½ FODO cells (157.16 m), followed by two 90° cells of horizontal dispersion suppression
- Another long section of 7 FODO cells (244.48 m), which includes a locally-achromatic insertion of 4 cells to complete horizontal alignment of the trajectory towards DUSEL plus create a vertical bend downwards of 150 mrad
- A final vertical 49 mrad bend upwards using triplet achromatic focusing
- A tunable triplet final focusing module to control beam size on the target

The first six quadrupoles in the LBNE beamline, plus Q105 and Q106 in NuMI, are powered individually to perform the optical match between the lattice functions of NuMI and those of the LBNE transfer line (8 optical constraints). Throughout this section β is kept small enough in both planes to avoid problems with the tight EPB apertures. This matching section is followed by 4½ 90° FODO cells characterized by quadrupoles Q213 through Q222. The cell length and phase advance are chosen to closely replicate the MI lattice. Within this section the elevation is gradually lowered and then leveled off at 16.20" above the MI BLC.

This first section of arc cells terminates in a MI-like dispersion suppressor (DS)[†]. The four subsequent FODO cells provide achromatic horizontal & vertical bending. Twelve rolled dipoles complete the horizontal alignment towards DUSEL, while each magnet simultaneously bends downwards by 12.5 mrad, generating a net vertical slope of 150 mrad. Design of the configuration comprising the compact DS plus bending achromat is driven partially to avoid conflicts between LBNE and the existing MI8 transfer line connecting the Booster with Main Injector. That LBNE and MI8 must co-exist at their crossing point is a consequence of the LBNE magnet installation & transportation scheme. Transporting magnets from the MI-8 Service Building to the upstream level region of LBNE dictates that LBNE & MI8 must have identical floor elevations (713.500 ft) [5].

[†] For 90° cells of length ℓ_{ARC} & bend θ_{ARC}, a compact MI-style suppressor is two 90° cells with $\ell_{DS} = 3/4 \cdot \ell_{ARC}$ & $\theta_{DS} = 2/3 \cdot \theta_{ARC}$.

DIPOLE TYPE (#)	L (m)	B (T)	TILT (deg)		QUAD NAME (#)	TYPE	L (m)	G (T/m)
NuMI EXTRACTION → LBNE								
6-3-120 (2)	3.048	1.62707	−90.000					
MATCH FROM NuMI → LBNE FODO LATTICE								
5-1.5-120 (3)	3.048	1.48162	+90.000		Q271→272 (2)	3Q60	1.524	+15.85427
					Q208	3Q120	3.048	−13.25194
					Q209	3Q120	3.048	+12.94503
					Q210	3Q120	3.048	−13.15068
IDA/B (1)	6.09981	1.62548	0.000		Q211	3Q120	3.048	+12.04974
					Q212	3Q120	3.048	−12.88347
FODO ARC CELLS								
IDA/B (8)	6.09981	1.62548	0.000		Q213→221 (9)	3Q120	3.048	±11.31286
LEVEL OFF 16.2" ABOVE MI ELEVATION								
IDA/B (2)	6.09981	1.65421	−10.688					
ARC CELLS								
IDA/B (9)	6.09981	1.62548	0.000					
MI-STYLE DISPERSION SUPPRESSOR								
IDC/D (8)	4.06654	1.62548	0.000		Q222	3Q120	3.048	−13.36379
					Q223→225 (3)	3Q120	3.048	±15.38716
					Q226	3Q120	3.048	−13.36379
FODO ACHROMATIC HORIZONTAL & VERTICAL BENDS								
IDA/B (12)	6.09981	1.43292	+34.950		Q227→233 (7)	3Q120	3.048	±11.31286
FODO STRAIGHT CELLS								
					Q234→239 (7)	3Q120	3.048	±11.31286
ACHROMATIC VERTICAL BEND UP								
IDA/B (2)	6.09981	1.60772	−90.000		Q240	3Q120	3.048	−13.30132
					Q241→242 (2)	3Q120	3.048	+13.96613
						3Q60	1.524	
					Q243→245 (3)	3Q60	1.524	−15.79799
					Q246→247 (2)	3Q60	1.524	+13.96613
						3Q120	3.048	
FINAL FOCUS ON TARGET WITH β* = 86.33 m [σ = 1.50 mm @ 120 GeV/c]								
					Q248	3Q120	3.048	−15.67642
					Q249	3Q120	3.048	+10.48725
					Q250	3Q60	1.524	−13.60648
					Q251	3Q120	3.048	−10.09757
					Q252	3Q120	3.048	+14.32797
					Q253	3Q120	3.048	− 5.51582

Table 1: Magnet parameters of the LBNE proton beamline at 120 GeV/c and β*=64.842 m

MI8 crosses the LBNE line immediately downstream of Q227 (refer to Figure 1). The compact DS design, coupled with the achromatic insertion, makes it possible to open a 6 m drift space at the crossing point without increasing the overall beamline length or disrupting the periodic focusing nature of the lattice. The 150 mrad vertical bend downwards begins with the 2 magnets in the half-cell upstream of MI8. At the entrance to the down bends LBNE BLC is 14.625" above that of MI8. At the intersection of the lines LBNE is descending with a 25 mrad slope and the BLC separation is reduced to 4.125". This leaves a completely adequate 0.125" of pipe-to-pipe clearance between the lines, and floor elevation is not impacted.

Following the FODO achromatic insertion the beam trajectory continues downwards at 150 mrad through 3 empty FODO cells. An achromatic vertical bend upwards of 49 mrad then establishes the final beam trajectory at the target. Quadrupoles Q248 through Q253 form the final focus (FF) optics to obtain the desired beam size at the target. This final focus is tunable to produce a spot size of σ = 1.00-3.00 mm over the entire momentum range 60-120 GeV/c.

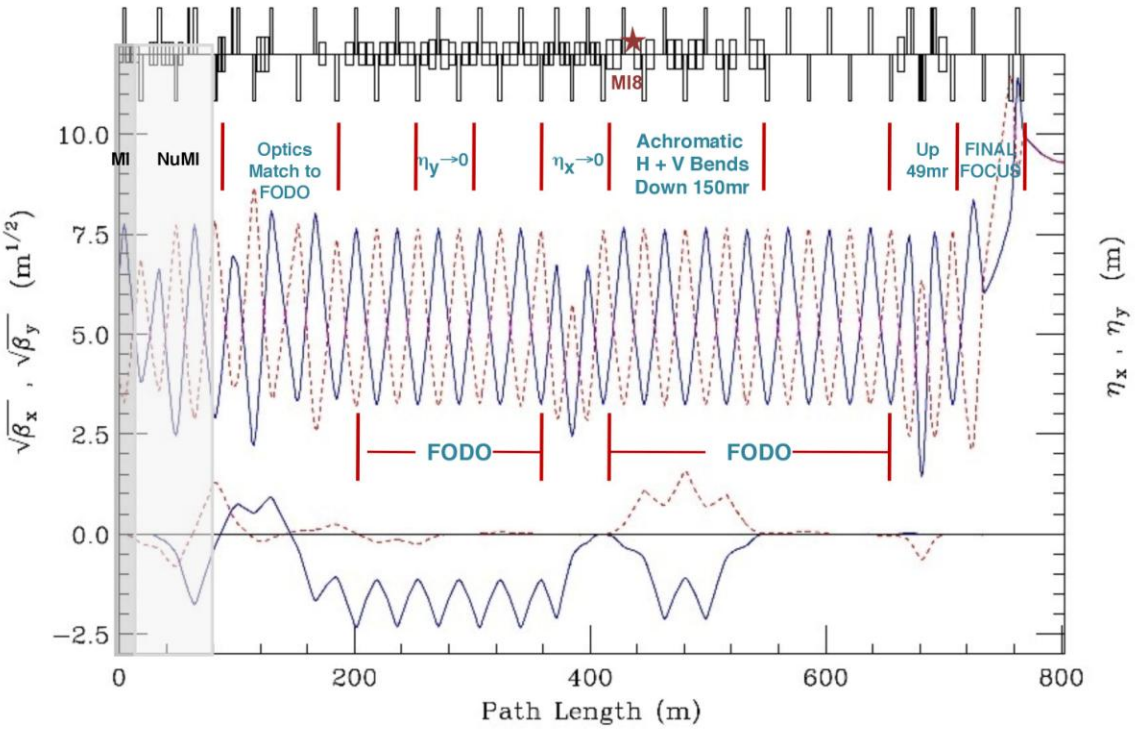

Figure 1: Horizontal (solid) and vertical (dashed) lattice functions of the LBNE transfer line
The final focus is tuned to produce a spot size of $\sigma_x = \sigma_y$ = 1.50 mm at 120 GeV/c and $\varepsilon = 26\pi$ μm (98%, normalized)

Magnet apertures (including the impact of rolls) and beam envelopes are shown in Figure 2. One contour corresponds to nominal MI beam parameters of $\varepsilon = 26\pi$ μm (98%, normalized) and $\Delta p_{98}/p$ = 9.e-4. The larger envelope shown is calculated for $\varepsilon = 360\pi$ μm (100%, normalized) and $\Delta p_{100}/p$ = 28.e-4. The latter values reflect the admittance of the Main Injector at transition (γ_t = 21.600), and the transfer of such a beam to LBNE could only result from a catastrophic failure of the MI and LBNE safety and regulatory systems. The maximum transverse emittance of 360π is determined by the restricted horizontal aperture in the Lambertson magnets seen by the circulating MI beam. The momentum spread is the maximum value that can be contained in a radio frequency bucket through acceleration. The $\varepsilon = 360\pi$ μm & $\Delta p_{100}/p$ = 28.e-4 envelopes, therefore, demonstrate that the LBNE beamline should be able to transport without losses the worst quality beam that the Main Injector could transmit.

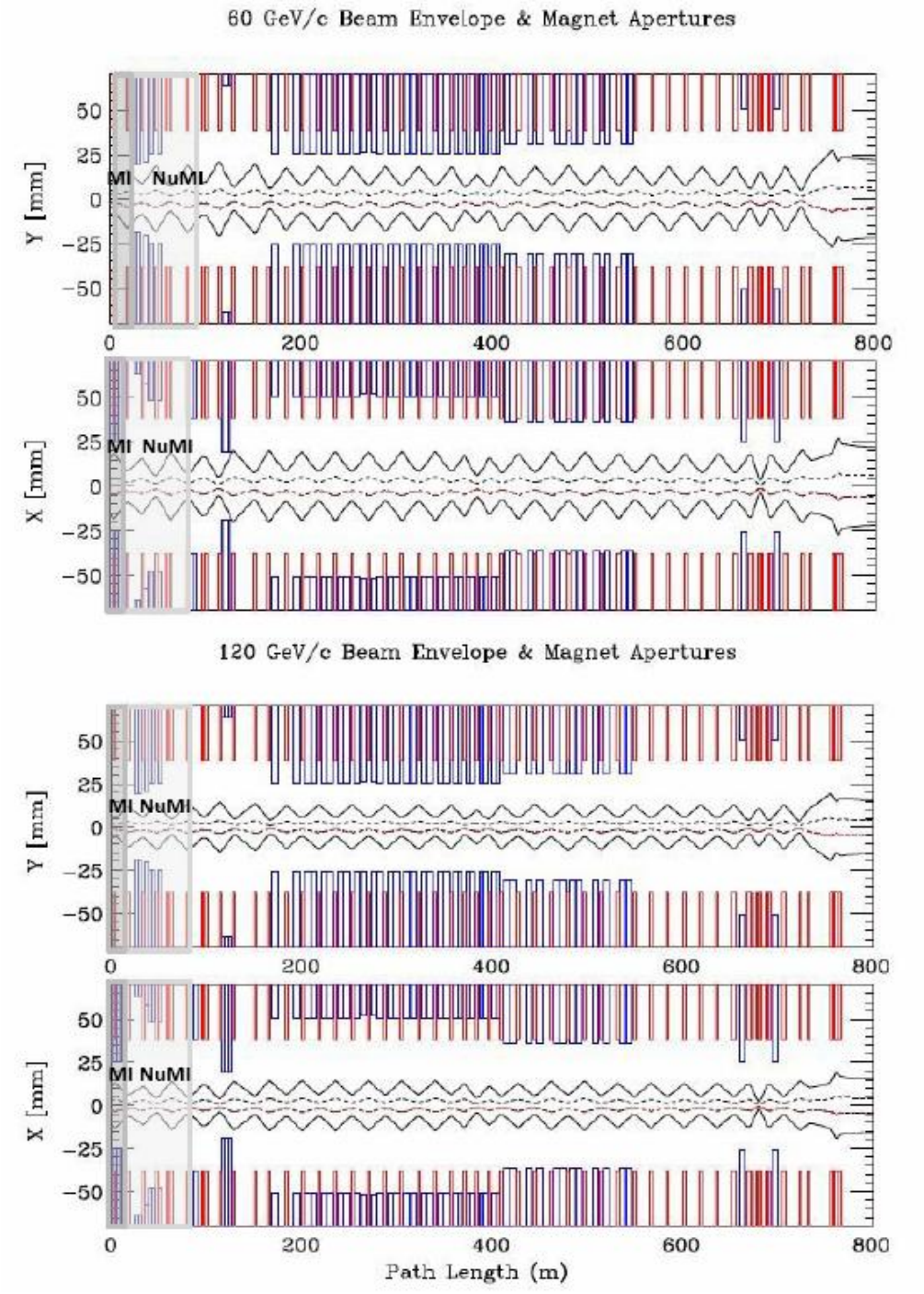

Figure 2: Magnet apertures and beam envelopes
The 98% contour (dashed) with nominal MI beam parameters, and; the 100% envelope (solid) corresponding to the MI admittance at transition (γ_t = 21.600).

Sensitivity to Gradient Errors

There is every reason for confidence that the optical integrity of the LBNE beamline will not be compromised by magnet-to-magnet variations in the integrated quadrupole fields. Experience with the MI-style 3Q120 magnets has shown that these magnets are very high quality, with a spread in gradient errors on the order of $\sigma(\Delta G/G) \sim 0.08\%$ or less [6]. Such a narrow error distribution cannot appreciably impact the beam characteristics or transport capabilities. Implementing even the most rudimentary strategy for sorting production quadrupoles, such as selecting those from the middle of the distribution for installation in the FODO cells, will reduce the spread even further. For nominal beam parameters at 120 GeV/c, a simple thin-lens calculation predicts that the largest error-wave expected in the 98% beam envelope ($\pm$3.48 mm nominal at β = 59.6 m) would be less than 65 microns.

Beam Size on Target

An essential design requirement of the final focusing section is the ability to tune the spot-size σ over a wide range. The optimum spot-size is thought to fall in the range σ ~1.5-2.0 mm, but this is still an evolving parameter. Ultimately, the choice will be driven to a large extent by details of the final target design, but other factors must also be considered. In addition to the 40% difference in beam size between 60 and 120 GeV/c, under real operational conditions the beam parameters (ε, $\Delta p/p$) will certainly be different from the ideal nominal values assumed here. Currently, the MI emittance at 120 GeV/c is ~20π, but it is not clear how this value might change in the future. It is essential that the FF design be sufficiently robust & versatile to anticipate these possibilities.

Figure 3 illustrates the wide tuning range of the FF. The two extreme results shown were calculated using nominal beam parameters, but the plot demonstrates that the FF should be adaptable to any reasonable set of beam parameters. The advantages of a modular optics design are evident — variations in the extracted MI beam parameters can be accommodated solely within the FF & do not involve alterations elsewhere in the line. Quadrupole gradients are listed in Table 3.

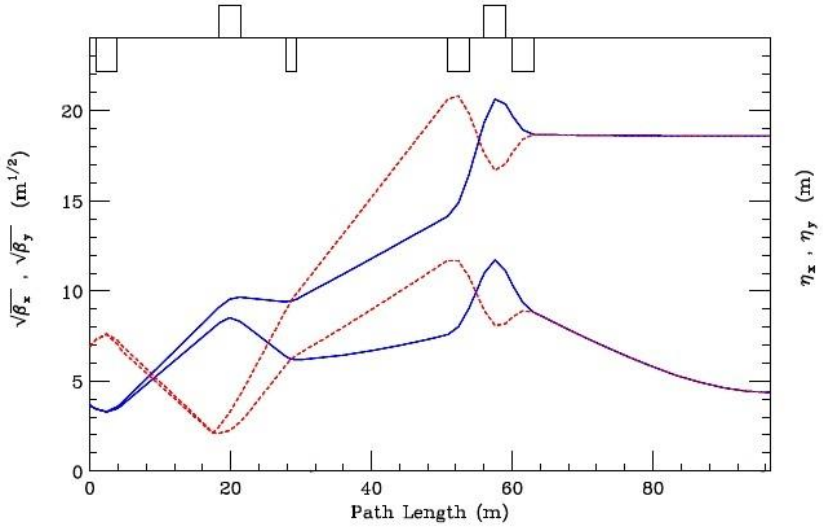

Figure 3: Tuning range of the Final Focus
These examples assume nominal MI beam parameters. At 60 GeV/c and σ = 1.0mm; β^* = 19.184m & βmax = 104m. At 120 GeV/c and σ = 3.00mm; β^* = 345 m & βmax = 460m.

			σ = 1.00mm @ 60 GeV/c β* = 19.184 m	σ = 3.00mm @ 120 GeV/c β* = 345.31 m
QUAD	TYPE	L (m)	G (T/m)	G (T/m)
Q248	3Q120	3.048	−15.67865	−18.1825
Q249	3Q120	3.048	+10.47574	+6.28358
Q250	3Q60	1.524	−13.02500	−6.66701
Q251	3Q120	3.048	−12.84453	−9.79837
Q252	3Q120	3.048	+19.74000	+13.14574
Q253	3Q120	3.048	−8.66527	−4.76765

Table 3: Final Focus gradients for the examples in Figure 3.

Trajectory Correction

Orbit correction is an issue which, of course, must be addressed in the design of any transfer line, but for the ultra-clean transport requirements of LBNE it is critical that precise position control be available throughout the beamline.

Correction of central trajectory errors have been simulated for dipole field errors and random misalignments assigned to all beamline elements (including BPM's). Realistic error values are on the order of $\sigma(\Delta_x,\Delta_y)$ = 0.25 mm, and $\sigma(\psi_{roll})$ = 0.50 mrad [7]. Figure 4 shows the trajectory deviations resulting from randomly generated Gaussian error distributions (dashed). After correction using the LBNE trim dipoles the new orbits are also shown (solid), emphasizing the dramatic reduction in offset errors. Results of the tracking are summarized in Table 4. All corrector strengths are well within the 250 μrad (60% of peak) design specification for the new IDS trims.

The (relatively) large residual value of Y_{max} is an artifact of the simulation model. For one random generator seed a badly misaligned quadrupole at the upstream end of the line caused this vertical spike, and the one or two available LBNE correctors had little impact. In reality, additional correctors upstream in NuMI could also be used for orbit control, or the quadrupole would simply be realigned. Beam position on the target is accurate to a few microns.

The fact that the orbit deviations are virtually the same in both planes indicates that quadrupole misalignments are the dominant source of errors. A 15 T/m quadrupole displaced transversely by 0.25 mm produces a kick ~30 μrad which is larger than the error angle resulting from ΔB/B = 10.E-4 in any of the beamline's dipoles.

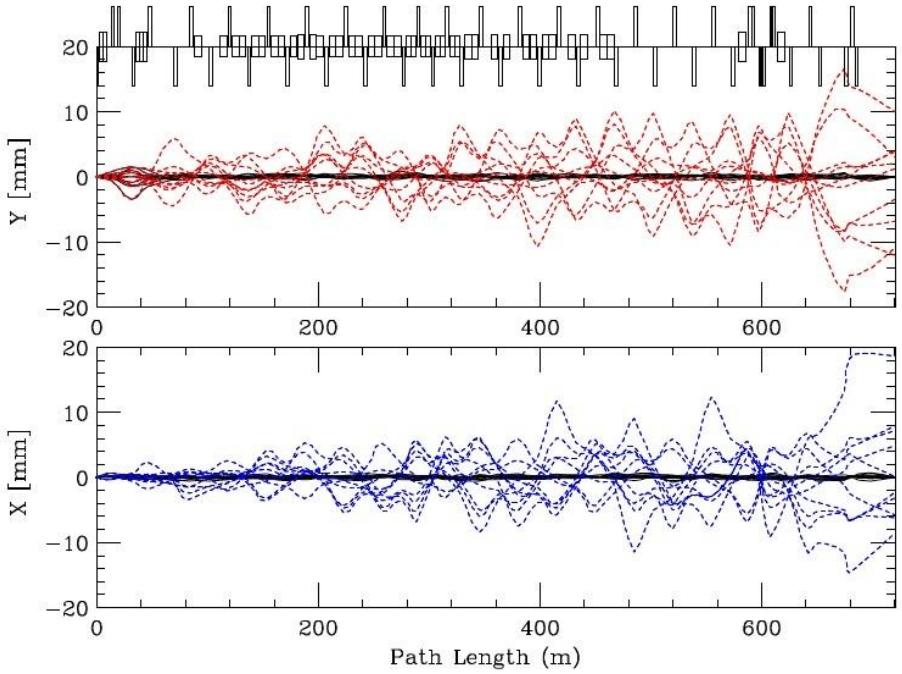

Figure 4: Uncorrected/corrected trajectories with random misalignments and dipole field errors The plot begins at mid-quad Q106 — the last quadrupole in the NuMI stub.

	ORBIT (mm)		CORRECTORS (μrad)		ORBIT (mm)		CORRECTORS (μrad)	
	X_{max}	X_{RMS}	θ_{max}	θ_{RMS}	Y_{max}	Y_{RMS}	φ_{max}	φ_{RMS}
UNCORRECTED	19.022	3.808	—	—	17.671	3.984	—	—
CORRECTED	0.795	0.253	78.582	28.068	3.451	0.352	121.467	34.156

Table 4: Orbit offsets and corrector kicks for the trajectories in Figure 4.

Summary

The LBNE beamline presented here is a modular optics design comprised of 5 distinct lattice configurations. In addition to the NuMI → LBNE matching section & Final Focus, three modules are designed specifically to compensate for abrupt changes in the beam trajectory. Perturbations generated in the lattice functions are locally corrected so they do not bleed out & corrupt the optics elsewhere in the line. Aperture studies indicate that the line is able to transport the worst quality beam that the Main Injector might provide. New IDS dipole correctors located at every focusing center provide high-quality orbit control & further ensure that the LBNE line meets the stringent requirements for environmental protection.

Acknowledgements

The authour welcomes this opportunity to thank his friends & colleagues in Accelerator Division, Technical Division, Mechanical Engineering, Alignment & Metrology, Electrical Engineering, and the LBNE Project Management for their valuable input & many entertaining discussions. Special thanks are owed to the LBNE Document Manager, Amelia, for her adept navigation through the arcane backwaters & bogs of word formatting.

References

[1] "LBNE Conceptual Design Report (vol. 2) – Neutrino Beamline", Sub-section 2.2.2.1.
[2] Ibid., Sub-section 2.2.2.4 & 2.2.2.5.
[3] Ibid., Sub-section 2.2.2.6.
[4] Ibid., Sub-section 2.5.2.1.
[5] Ibid., Sub-section 2.2.2.7.
[6] David Harding (private communication) and; Magnet Test Facility measurement database.
[7] Virgil Bocean (private communication) and; John A. Johnstone, "A Modular Optics Design for the NuMI Beamline", Fermilab-TM-2174 (and references therein).

Ω